

Supplementary information

Preparation and characterization of novel polyoxometalate/CoFe₂O₄/metal–organic framework magnetic core-shell nanocomposites for rapid removal of organic dyes from water

Afsoon Jarrah and Saeed Farhadi*

Department of Chemistry, Lorestan University, Khorramabad, 68151-44316, Iran

*Corresponding author: E-mails: farhadi.s@lu.ac.ir

Equations used for thermodynamic and kinetic models in this work:

$$\frac{C_e}{q_e} = \frac{C_e}{q_m} + \frac{1}{q_m K_L} \quad (\text{Eq. S1})$$

Where K_L , q_m , and C_e are the Langmuir constant (mg l^{-1}), high adsorption capacity (mg g^{-1}), and the equilibrium concentration of pollutant solution (mg l^{-1}), respectively, that q_m and K_L were calculated from the intercept and slope of isotherm plots.

$$R_L = \frac{1}{1 + K_L C_0} \quad (\text{Eq. S2})$$

Where C_0 is the primary dye concentration, the R_L factor offers the kind of the isotherm to be favorable ($0 < R_L < 1$), irreversible ($R_L = 0$), linear ($R_L = 1$), or unfavorable ($R_L > 1$ or $R_L < 0$).

$$\text{Log} q_e = \text{Log} k_f + \frac{1}{n} \cdot \text{Log} C_e \quad (\text{Eq. S3})$$

Where n and K_f (mg/g) indicate heterogeneity factor and Freundlich constant connecting to the adsorption intensity and capacity, respectively.

$$\ln(q_e - q_t) = \ln q_e - k_1 t \quad (\text{Eq. S4})$$

$$\frac{t}{q_t} = \frac{1}{k_2 q_e^2} + \frac{1}{q_e} t \quad (\text{Eq. S5})$$

$$q_t = k_p t^{\frac{1}{2}} + I \quad (\text{Eq.S6})$$

Where q_t and q_e (mg/g) are the concentrations of dye adsorbed at any time t and equilibrium time (min), respectively. k_1 (min^{-1}) and k_2 ($\text{g mg}^{-1}\text{min}^{-1}$) are the rates constants of adsorption for the pseudo-first-order and the pseudo-second-order models respectively, and k_p ($\text{mg/g}^{-1}\text{min}^{-1}$) and I are the intraparticle dissemination rate constant and intercept for the first linear phase.

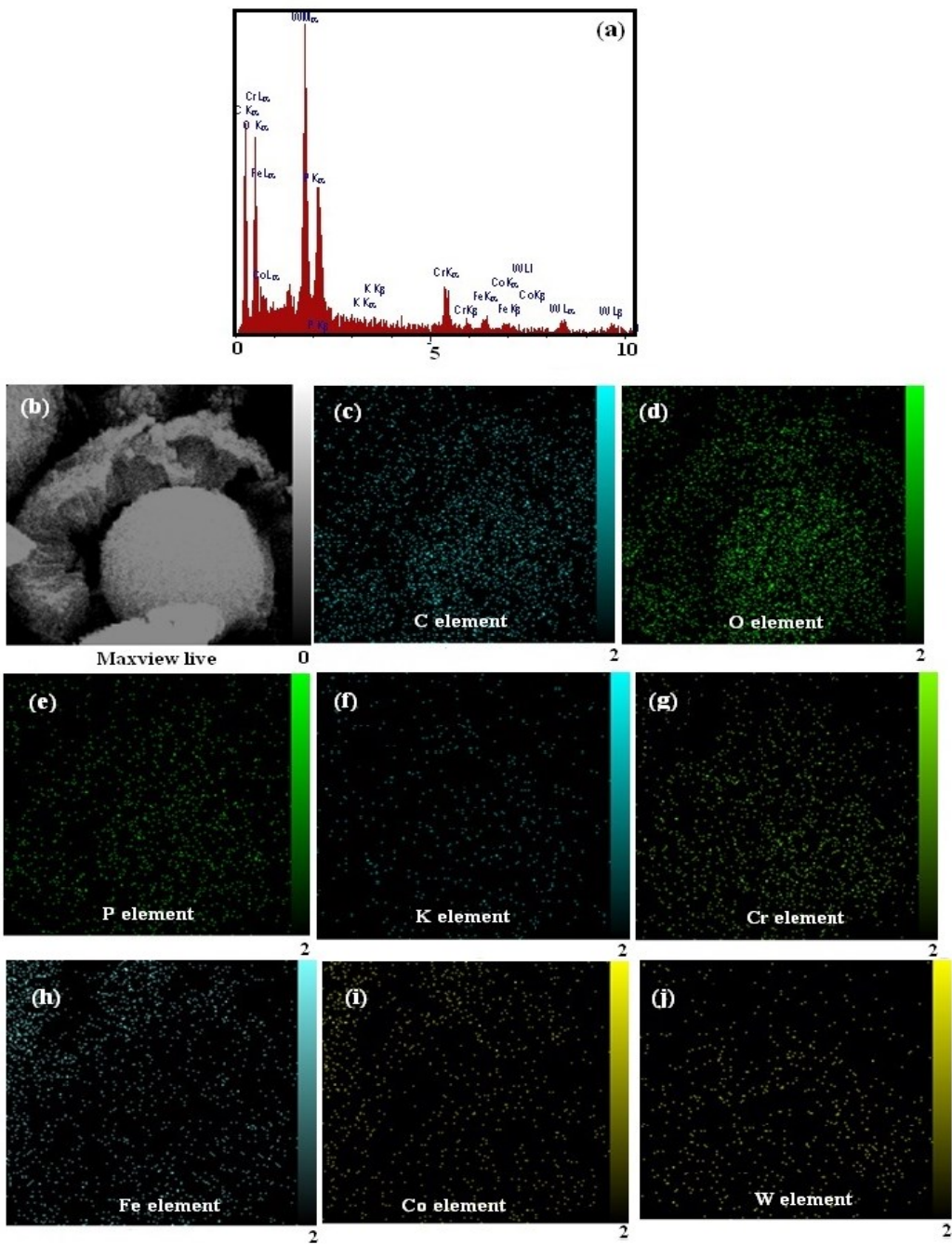


Fig. S1. EDX spectrum (a) and a representative SEM image of the POM/CFO/MIL-101(Cr) (b) with corresponding EDX elemental mappings (c)-(j).

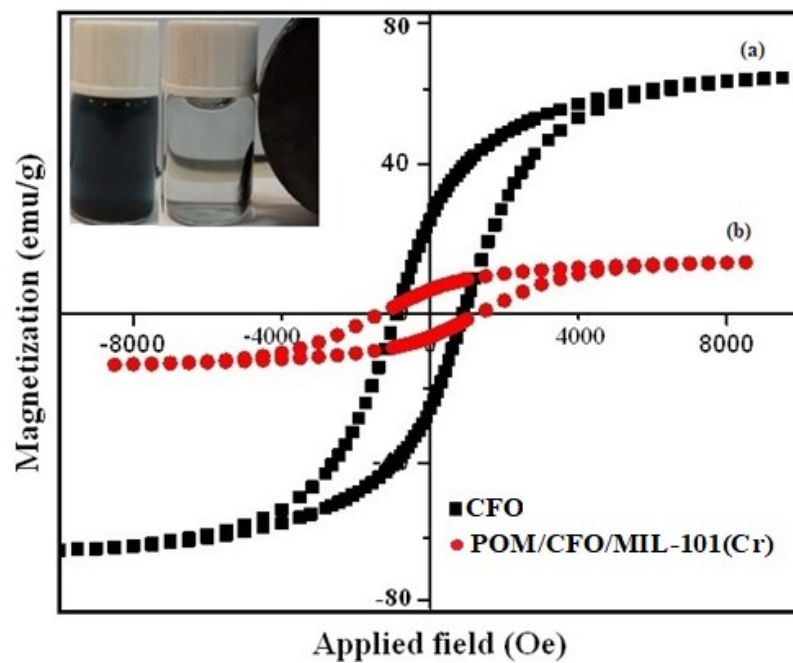


Fig. S2. Magnetization curves of CFO (a) and POM/CFO/MIL-101(Cr) (b). The inset shows the use of an outer magnetic field to separate the POM/CFO/MIL-101(Cr) sample.

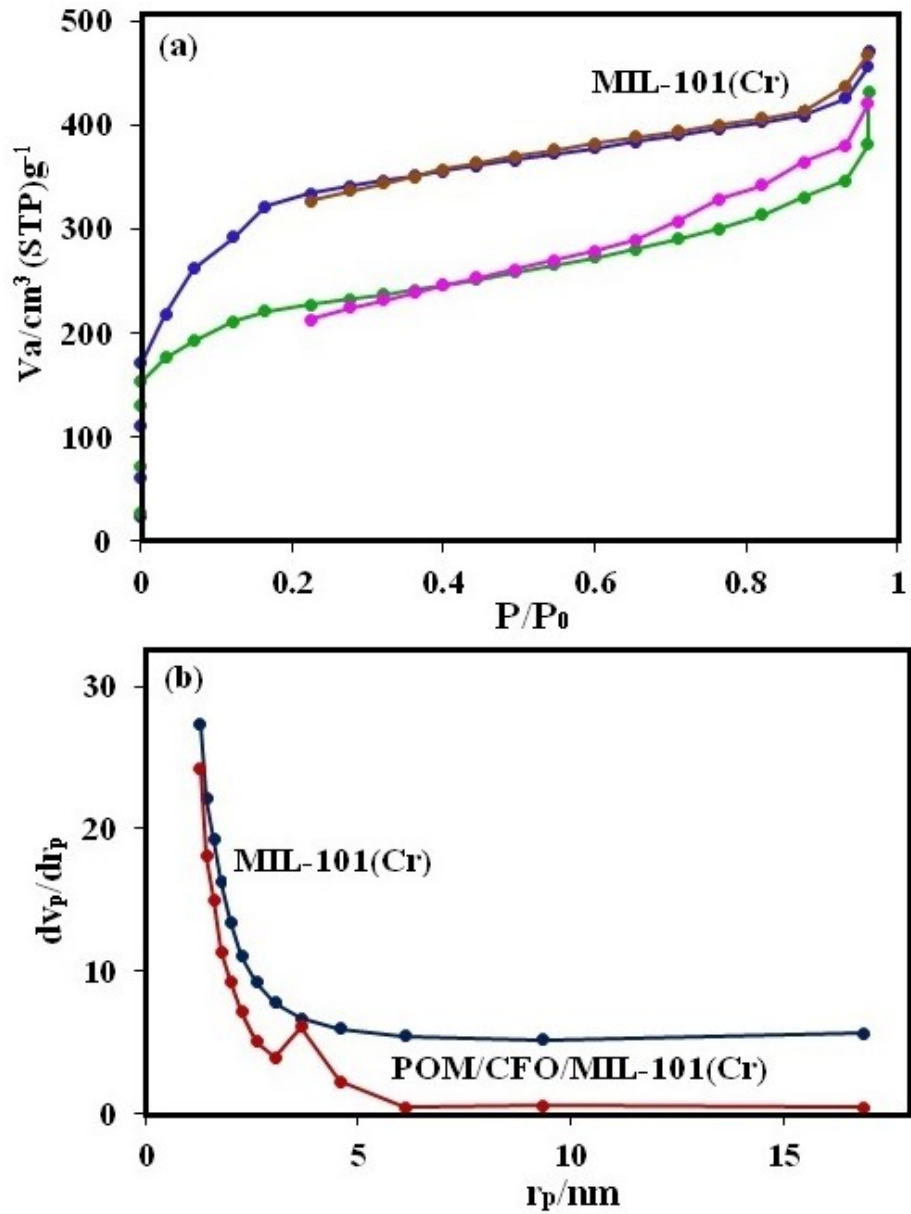


Fig. S3. BET isotherms (a) and pore size distributions of MIL-101(Cr) and POM/CFO/MIL-101(Cr) samples.

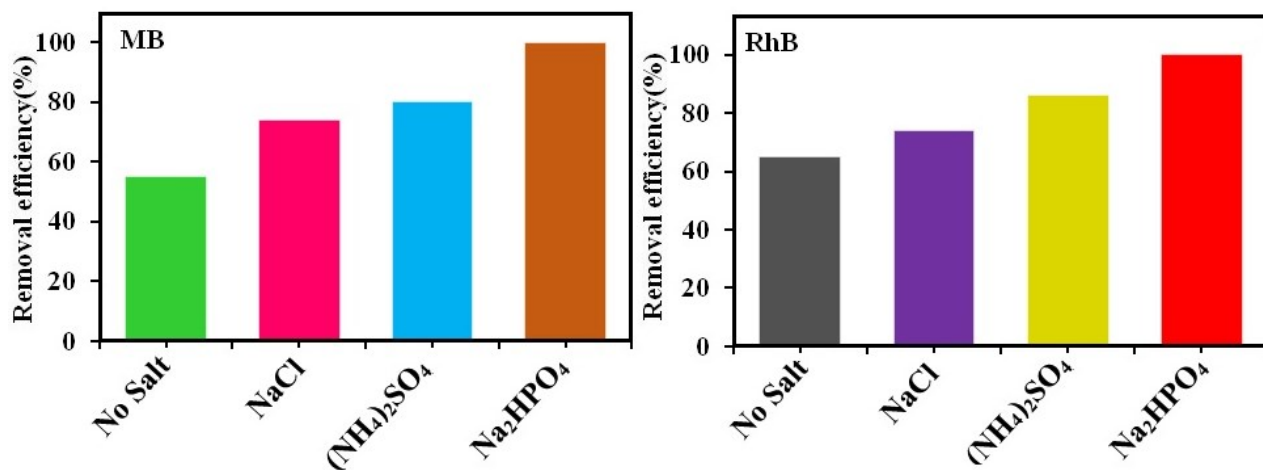


Fig S4. the effect of salt on the dye adsorption by the POM/CFO/MIL-101(Cr). Conditions: $C_{0(\text{MB})} = 100$ mg/L, $C_{0(\text{RhB})} = 50$ mg/L, adsorbent dose = 30 mg, pH = 6 and temp. = 25 °C. The contact adsorption times for MB and RhB dyes were 20 and 25 min, respectively.

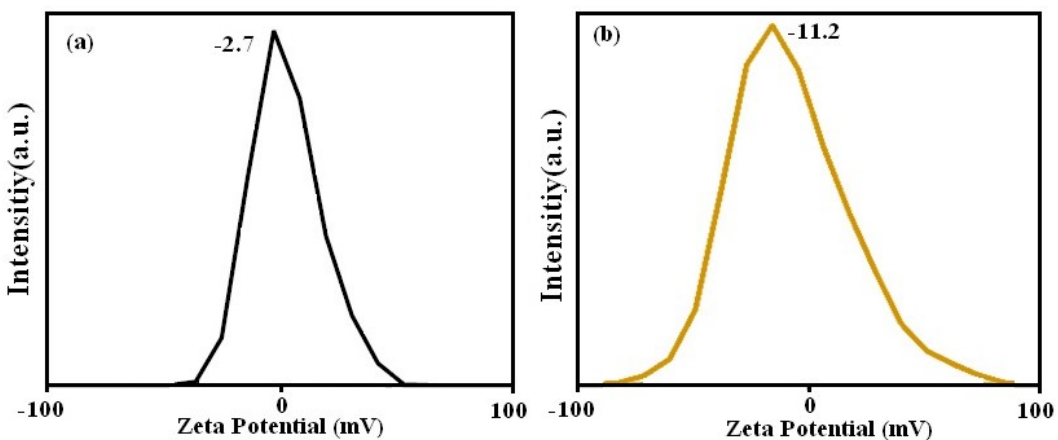


Fig. S5. Zeta potential curves of (a) pure MIL-101 and (b) P₂Mo₁₈/MIL-101 (Cr) in aqueous solutions at natural pH of about 6.5.

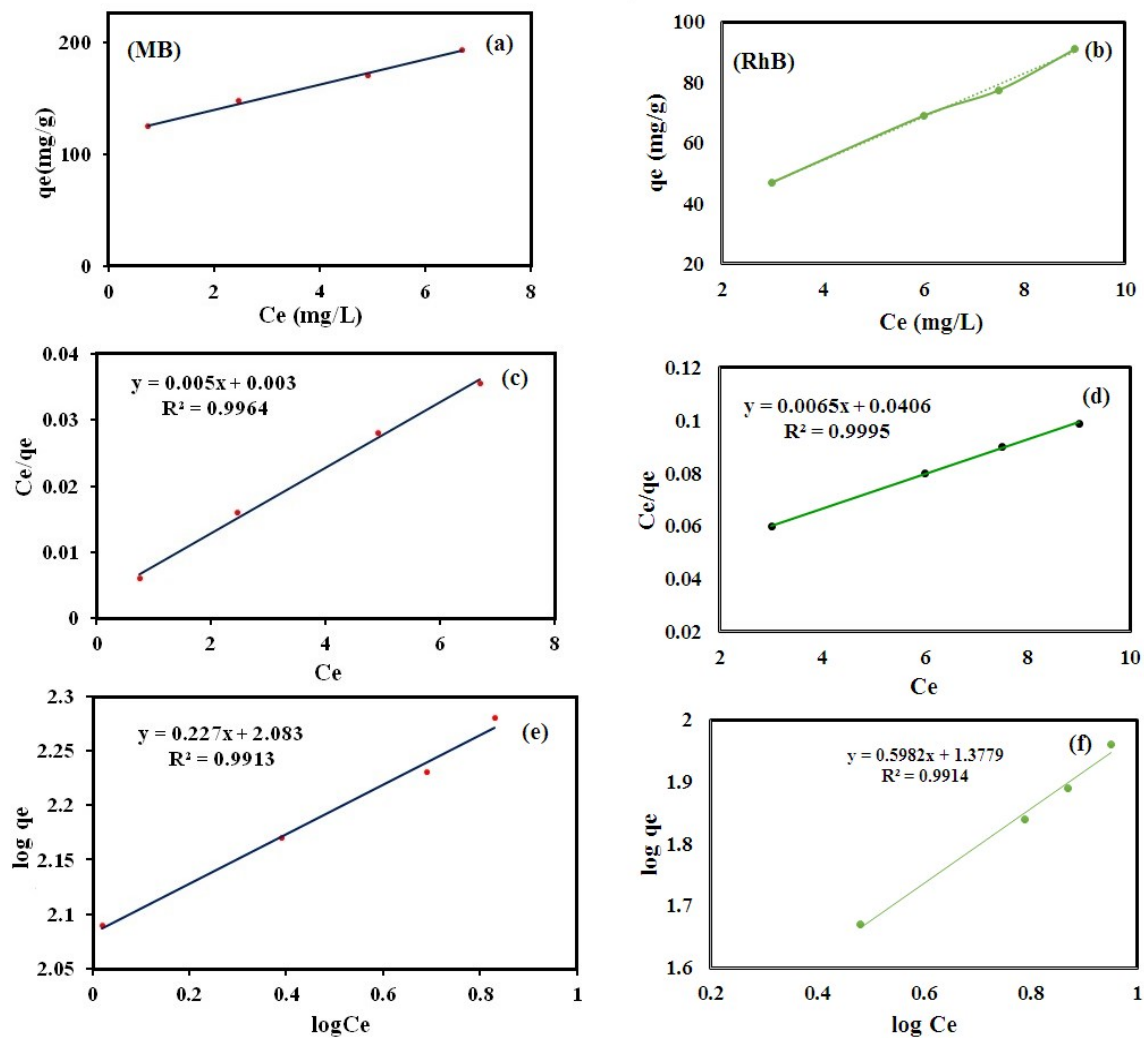


Fig. S6. Adsorption isotherm curves of (a) MB and (b) RhB, onto POM/CFO/MIL-101(Cr), (c, d) Langmuir, and (e, f) Freundlich isotherms.

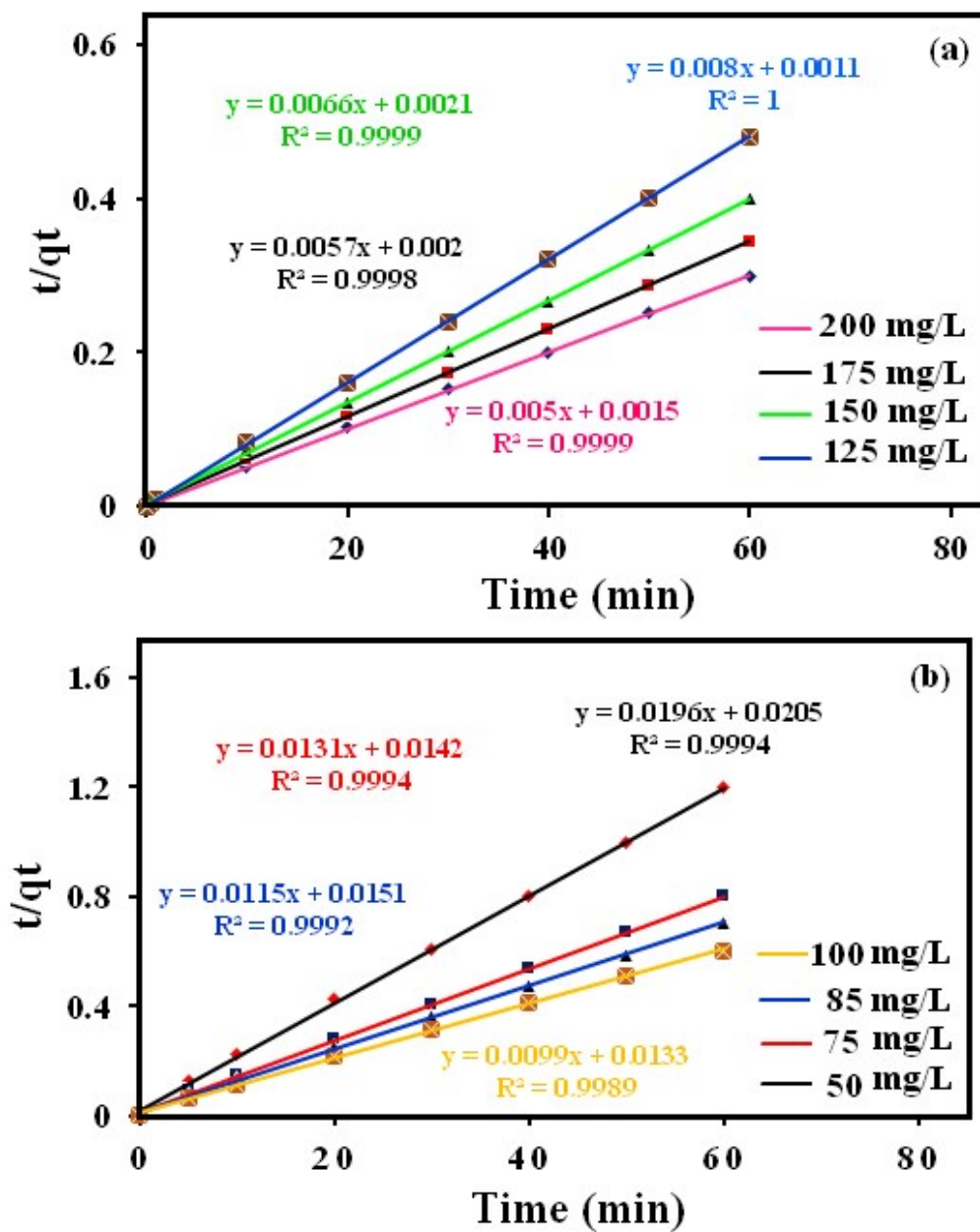


Fig. S7. Pseudo-second order kinetics for MB (a) and RhB (b) adsorptions.

Table S1. Comparison of adsorption performance of various adsorbents for MB.

Adsorbent	Adsorption capacity (mg/g)	C_{MB} (mg L ⁻¹)	Time	Ref.
H ₆ P ₂ W ₁₈ O ₆₂ /MOF-5	51.81	10	10 min	[48]
MOF/GO	183.4	36	30 min	[49]
Mesoporous MIL-101	22.5	30	2 h	[50]
MOF-235	187	300	12 h	[51]
H ₃ PW ₁₂ O ₄₀ @Mn ^{III} porphyrin	10.5	10	24 h	[52]
MOF-Cu-BTC	15.28	3.19	6 h	[53]
H ₆ P ₂ W ₁₈ O ₆₂ @Cu ₃ (BTC) ₃	18.51	40	1 h	[54]
Carbon nanotubes	35.4	35	50 min	[55]
Activated carbon	135	60	10 min	[56]
Exfoliated graphene oxide	17.3	30	80 min	[57]
Nano-ZIF - 8	126	60	30 min	[58]
H ₃ PW ₁₂ O ₄₀ / ZIF-8	298	60	30min	[58]
H ₃ PW ₁₂ O ₄₀ /MIL-101(Fe)	473.7	100	5 min	[59]
H ₄ PW ₁₁ V/MIL-101(Cr)	371	100	30 min	[60]
PV ₂ Mo ₁₀ -M(membrane)	82	20	-	[61]
Graphene oxide	397	34.8	25 min	[62]
Zn-DDQ	135	500	70 min	[63]
MIL-100(Fe)	736	30	90 min	[64]
ErCu-POM(Er-3)	391	20	-	[65]
POM/CFO/MIL-101(Cr)	200	100	23 min	This work